IET Electrical Systems in Transportation

Research Article

IET Journals
The Institution of Engineering and Technology

Off-board electric vehicle battery charger using PV array

ISSN 2042-9738
Received on 31st January 2019
Revised 8th February 2020
Accepted on 27th March 2020
E-First on 30th April 2020
doi: 10.1049/iet-est.2019.0035
www.ietdl.org

Sujitha Nachinarkiniyan[1], Krithiga Subramanian[1] ✉

[1]*School of Electrical Engineering, Vellore Institute of Technology, Chennai 600 127, Tamil Nadu, India*

✉ *E-mail: s_krithiga@yahoo.com*

Abstract: During the recent decade, the automobile industry is booming with the evolution of electric vehicle (EV). Battery charging system plays a major role in the development of EVs. Charging of EV battery from the grid increases its load demand. This leads to propose a photovoltaic (PV) array-based off-board EV battery charging system in this study. Irrespective of solar irradiations, the EV battery is to be charged constantly which is achieved by employing a backup battery bank in addition to the PV array. Using the sepic converter and three-phase bidirectional DC–DC converter, the proposed system is capable of charging the EV battery during both sunshine hours and non-sunshine hours. During peak sunshine hours, the backup battery gets charged along with the EV battery and during non-sunshine hours, the backup battery supports the charging of EV battery. The proposed charging system is simulated using Simulink in the MATLAB software and an experimental prototype is fabricated and tested in the laboratory and the results are furnished in this study.

1 Introduction

Ever increasing effects of green house gases from the conventional IC engines lead to environmental concerns. This paved to the booming of pollution free electric vehicles (EVs) in the automobile industry [1–3]. However, EV battery charging from the utility grid increases the load demand on the grid and eventually increases the electricity bills to the EV owners which necessitate the use of alternate energy sources [4, 5]. Due to inexhaustible and pollution free nature of renewable energy sources (RESs), it can be used to charge the EV battery. Thus, RES driven EV can be termed as 'green transportation' [6]. Solar is one of the promising RESs which can be easily tapped to utilise its energy to charge EV battery [7, 8]. Hence, PV array power is used to charge the EV battery in the proposed system with the help of power converter topologies.

Lithium ion batteries are widely used in the EV due to its high power density, high efficiency, light weight and compact size [9, 10]. Also, these batteries have the capacity of fast charging and long lifecycle with low self-discharge rate. They also have low risk of explosion if it is over charged or short circuited. During charging, these batteries require precise voltage control. Hence, various power electronic converters with voltage controller are used for charging EV battery.

Due to the intermittent nature of the PV array, there is a need for power converters to charge the EV battery. Among different converters, multiport converters (MPCs) are preferred in the on-board chargers of hybrid EVs due to its capability of interfacing power sources and energy storage elements like PV array, ultracapacitors, super capacitors, fuel cells and batteries with the loads in EV like motor, lights, power windows and doors, radios, amplifiers and mobile phone charger. The MPCs have the drawback of increase in weight, cost and maintenance of the EV as all the sources are placed in the EV itself. Also, the complexity of controller implementation increases in these converter-based EV battery charging system [11–13]. Hence, an off-board charger is proposed in this paper in which the EV battery is located inside the vehicle unit and PV array and backup battery bank are located in the charging station or parking station. Various converter topologies for off-board charging system are presented in the literature [14–16].

Among different converter topology, the sepic converter is preferred due to its capability of working in both boost and buck modes. It also has the advantage of the same input and output voltage polarity, low input current ripple and low EMI [17, 18]. However, during low solar irradiation and non-sunshine hours, there is a need for an additional storage battery bank to charge the EV battery. This backup battery bank has to be charged in the forward direction and discharged in a reverse direction depending on the solar irradiation. Hence, a bidirectional converter with power flow in either direction is required [19].

The bidirectional converters are classified into non-isolated and isolated converters. Transformer in the isolated converters provides isolation which increases the price, weight and size of the converter. The main concerns of EV are weight and size and hence, non-isolated bidirectional converters are best suited for this application [20–22].

Among various non-isolated bidirectional converter topologies, bidirectional interleaved DC–DC converter (BIDC) is preferred due to its advantages like improved efficiency in discontinuous conduction mode and minimal inductance value, reduced ripple current due to multiphase interleaving technique. Snubber capacitor across the switches reduces the turnoff losses and the inductor current parasitic ringing effect is also reduced by employing zero voltage resonant soft switching technique. These are the added advantages of this bidirectional converter [23–25]. The system in [25] is an off-board EV battery charging system which charges the EV battery from PV array power through bidirectional DC–DC converter in stand-still condition and EV battery gets discharged to drive the dc load in the EV during the running condition. It has the drawback of charging EV battery only during sunshine hours. To overcome this disadvantage and to charge the EV battery without any interruption, the proposed charger is developed using PV array integrated with sepic converter, bidirectional DC–DC converter and backup battery bank for charging the battery of an EV.

2 Operation of the proposed system

The proposed PV-EV battery charger consists of a PV array, a sepic converter, a half-bridge BIDC, an EV battery, a backup battery bank and a controller as shown in Fig. 1. The controller is used to generate the gate pulses to the sepic converter for obtaining the constant output voltage at the dc link. The gate pulses to the switches of BIDC are also generated to operate BIDC in boost mode to charge the backup battery from PV array and in buck

mode to charge EV battery from the backup battery. Also, the controller generates the gate pulses to the auxiliary switches S_a, S_b and S_c. During high solar irradiation, all the auxiliary switches are ON to interface dc link with PV array through the sepic converter, dc link with the backup battery through BIDC and dc link with EV battery. When solar irradiation is low, switch S_a is turned OFF isolating the PV array and sepic converter from the dc link. Whereas the switch S_c is turned OFF to disconnect BIDC and backup battery from the dc link, when the solar power is insufficient to charge backup battery. The proposed system operates in three modes viz., mode 1, mode 2 and mode 3 as explained in this section.

2.1 Mode 1

During peak sunshine hours, when the generated PV array power is higher, all the auxiliary switches are ON to charge both EV battery and backup battery simultaneously from PV array through sepic converter and BIDC, respectively. In this mode, BIDC operates in forward direction boosting the dc link voltage to charge backup battery.

2.2 Mode 2

During low solar irradiation conditions and non-sunshine hours, PV array power is insufficient to charge EV battery. Hence, the PV array is disconnected from the dc link by turning OFF the switch S_a and switches S_b & S_c are ON connecting EV battery to the backup battery through BIDC. In this mode, BIDC operates in reverse direction stepping down the backup battery voltage to charge EV battery.

2.3 Mode 3

When PV array power generated is sufficient to charge only EV battery, switches S_a and S_b are ON and switch S_c is OFF to disconnect the BIDC and backup battery bank from the dc link.

3 Design of the converters used in the proposed charger

3.1 Sepic converter

In the proposed charging system, the sepic converter provides the constant output voltage irrespective of the PV array voltage by adjusting its duty ratio using the PI controller. The sepic converter consists of one IGBT switch, one diode, two inductors and two capacitors as shown in Fig. 2. The major advantages of the sepic converter are: (i) it can operate in both boost and buck modes depending on the duty ratio; (ii) it provides the output voltage with the same polarity as input voltage unlike buck–boost and cuk converters [16]. The voltage gain of the sepic converter is provided by the following equation:

$$\frac{V_{\mathrm{dc}}}{V_{\mathrm{PV}}} = \frac{D}{1-D} \tag{1}$$

where V_{dc} is the dc link voltage, V_{PV} is the PV array voltage and D is the duty ratio of the sepic converter. The values of inductors and capacitors of the sepic converter are chosen as per (2)–(4) [17]:

$$L_a = L_b = \frac{V_{\mathrm{PVmin}} D_{\max}}{2\Delta i_{\mathrm{PV}} f_{\mathrm{sw}}} \tag{2}$$

$$C_1 = \frac{I_{\mathrm{dc}} D_{\max}}{\Delta V_{C1} f_{\mathrm{sw}}} \tag{3}$$

$$C_2 = \frac{I_{\mathrm{dc}} D_{\max}}{\Delta V_{\mathrm{dc}} f_{\mathrm{sw}}} \tag{4}$$

where V_{PVmin} is the minimum PV array voltage, Δi_{PV} is the input current ripple, f_{sw} is the switching frequency, I_{dc} is the dc link current, ΔV_{C1} is the capacitor, C_1 voltage ripple, ΔV_{dc} is the output voltage ripple, and $D_{\max}$ is the maximum duty ratio calculated as follows:

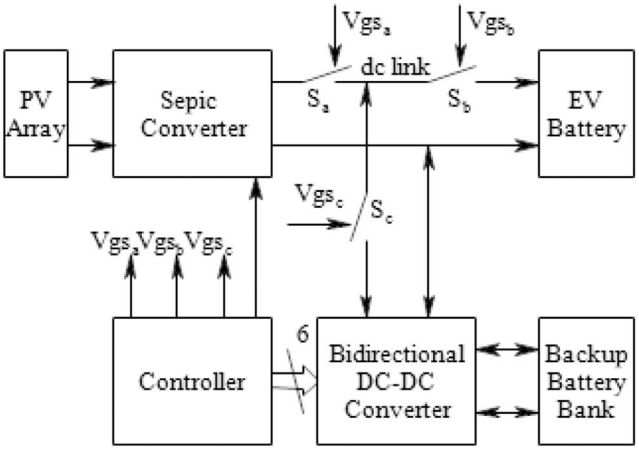

Fig. 1 *Block diagram of the EV battery charger*

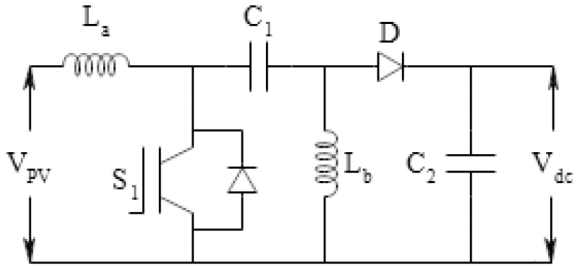

Fig. 2 *Schematic diagram of sepic converter*

$$D_{\max} = \frac{V_{\mathrm{dc}} + V_D}{V_{\mathrm{PVmin}} + V_{\mathrm{dc}} + V_D} \tag{5}$$

where V_{D} is the diode voltage drop.

3.2 Bidirectional interleaved DC–DC converter

Fig. 3 shows the schematic diagram of the BIDC employed in the proposed charging system. Backup battery bank is located on the high voltage side while the dc link is on the low voltage side of the converter. This converter operates in boost mode in forward direction and in buck mode in reverse direction. In boost mode, switches S_{L1}, S_{L2} and S_{L3} are the active switches whereas, in buck mode, the active switches are S_{U1}, S_{U2} and S_{U3}. There is an anti-parallel diode and parallel snubber capacitor to all the switches employed in this converter. In boost mode, the inductors L_1, L_2 and L_3 act as boost inductors whereas they act as a low-pass filter in buck mode. The capacitors, C_L and C_H are the smoothing energy buffer elements of this converter. Interleaved inductor currents minimise the ripples in the current. The modes of operation of the converter are analysed by considering the operation of a single leg converter in [20]. The voltage conversion ratio of BIDC in boost and buck modes are given by (6) and (7), respectively

$$\frac{V_{\mathrm{BackupBatt}}}{V_{\mathrm{dc}}} = \frac{1}{1-D_{\mathrm{Boost}}} \tag{6}$$

$$\frac{V_{\mathrm{dc}}}{V_{\mathrm{BackupBatt}}} = D_{\mathrm{Buck}} \tag{7}$$

where $V_{\mathrm{BackupBatt}}$ is the backup battery voltage and D_{Boost} is the duty ratio of BIDC in boost mode and D_{Buck} is the buck mode duty ratio. The values of inductors are considered less than the critical inductance values in both boost and buck modes to operate the converter in discontinuous conduction mode to improve efficiency

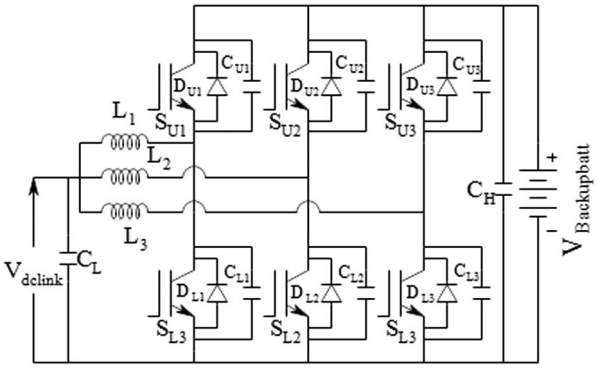

Fig. 3 *Schematic diagram of half-bridge BIDC*

[20]. The critical inductance value is calculated in boost and buck modes using (8) and (9), respectively

$$L_{\text{cric}} = \frac{3V_{\text{BackupBatt}}^2 D_{\text{Boost}}(1 - D_{\text{Boost}})^2}{2Pf_s} \tag{8}$$

$$L_{\text{cric}} = \frac{3V_{\text{dc}}^2(1 - D_{\text{Buck}})}{2Pf_s} \tag{9}$$

where P is the Backup battery power. The values of the capacitors on the low and high voltage side of BIDC are considered based on the following equations:

$$C_H = \frac{D_{\text{Boost}}P}{2f_s V_{\text{BackupBatt}}^2} \tag{10}$$

$$C_L = \frac{V_{\text{BackupBatt}} D_{\text{Buck}}(1 - D_{\text{Buck}})}{8f_s^2 L \Delta V_{\text{dc}}} \tag{11}$$

4 Design of controllers

Controller of the proposed charger generates gate pulses to the switches present in the sepic converter, BIDC and also to the three auxiliary switches. The algorithm to turn ON and turn OFF the auxiliary switches is shown in Fig. 4. Controller senses the PV array voltage and current, and computes the PV array power. If the PV array power is greater than EV battery rated power, P_{R}, then the controller generates the gate pulses to turn ON all the auxiliary switches to charge both EV battery and backup battery bank simultaneously from the PV array. If the PV array power is lesser than EV battery rated power but higher than the minimum required power, P_{M}, the switch, S_c is turned OFF disconnecting the backup battery from the charging system and switches, S_a and S_b are turned ON to charge the EV battery alone from the PV array. If the PV array power is lesser than the minimum required power, P_{M}, then the switch, S_a is turned OFF to isolate the PV array and sepic converter from the charging system. The switches, S_b and S_c are turned ON enabling the backup battery to charge EV battery. The PI voltage controller is used in the proposed charging system to generate gate pulses to the MOSFET in the sepic converter to maintain a constant voltage at the dc link irrespective of variations in the PV array voltage.

BIDC comprises of three legs with two switches in each leg. Gate pulses have to be provided to the two switches in the same leg with the phase shift of 180° from each other. The controller in the proposed system generates six gate pulses to the BIDC depending on the PV array power. If PV array power exceeds P_{R}, gate pulses are generated to the switches of BIDC to operate it in boost mode, stepping up the dc link voltage to charge the backup battery bank. In this mode, the gate pulses are generated to the switches of leg 1 with 0° phase and to the leg 2 switches with 120° phase shift from that of leg 1 switches and to the leg 3 switches with 240° phase shift from that of leg 1 switches. If the PV array power is less than P_{M}, the gate pulses are generated accordingly to operate BIDC in buck mode, producing a step down voltage at the dc link sufficient to charge the EV battery by the backup battery. In this mode, the gate pulses are fed to the leg 3 switches with 0° phase and gate pulses to the leg 2 and leg 1 switches are 120° and 240° phase shifted with respect to that of leg 3 switches, respectively.

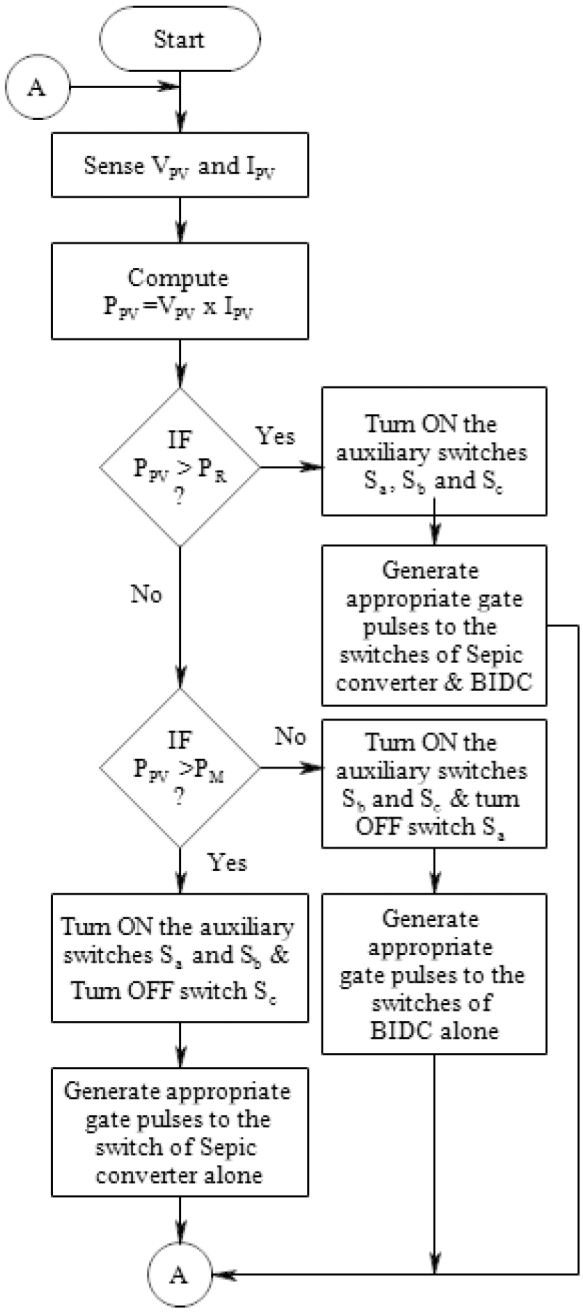

Fig. 4 *Flowchart of gate pulses generation for the auxiliary switches*

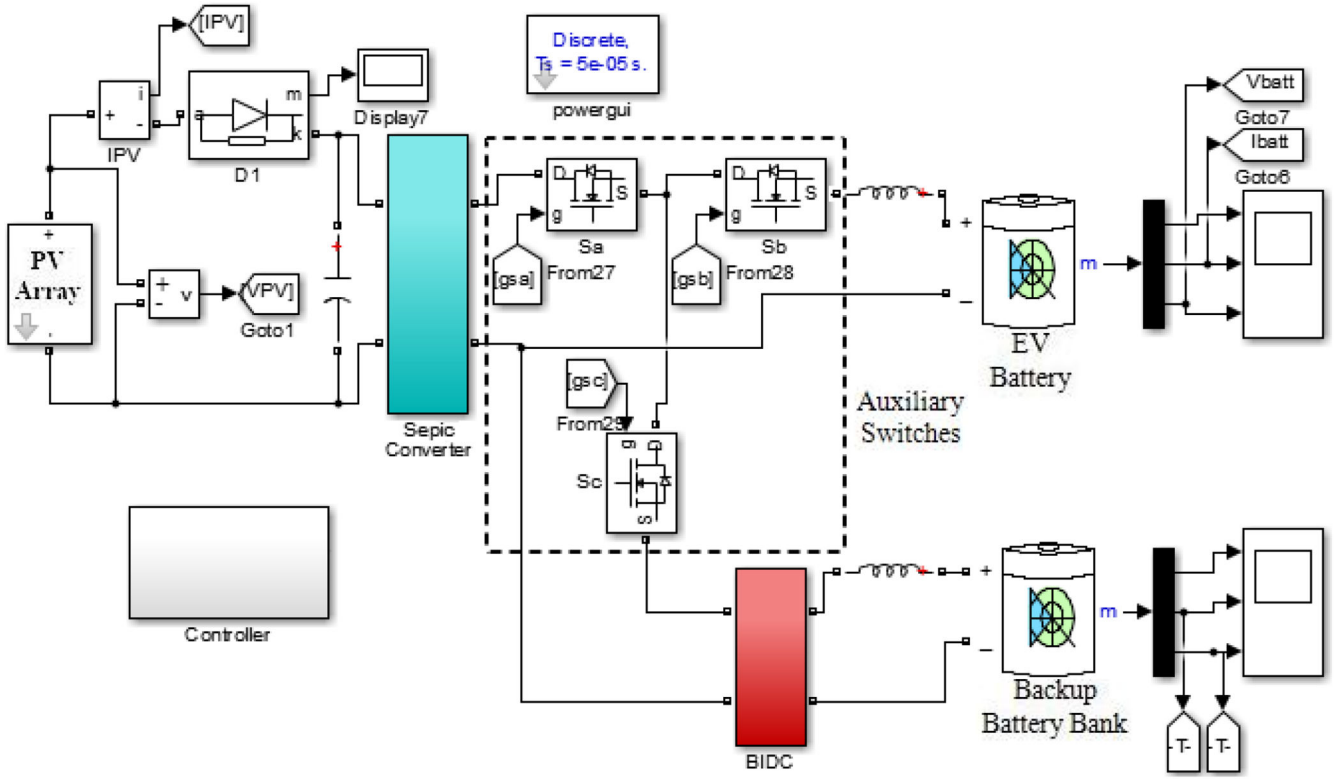

Fig. 5 *Simulation model of the proposed charger*

5 Mathematical modelling of proposed system

Mathematical model of the proposed system is obtained by combining the state-space average model of Sepic converter and Bidirectional DC–DC converter. It is derived by considering the ON and OFF switching period of the converters [26, 27]. The state-space matrices of the sepic converter, state matrix '$\boldsymbol{A}$', input matrix '$\boldsymbol{B}$', output matrix '$\boldsymbol{C}$', feed forward matrix '$\boldsymbol{D}$' are found to be

$$\boldsymbol{A}=\begin{bmatrix} 0 & 0 & \dfrac{-(1-D_{\mathrm{s}})}{L_a} & \dfrac{-(1-D_{\mathrm{s}})}{L_a} \\ 0 & 0 & \dfrac{D_{\mathrm{s}}}{L_b} & \dfrac{-(1-D_{\mathrm{s}})}{L_b} \\ \dfrac{(1-D_{\mathrm{s}})}{C_1} & \dfrac{-D_{\mathrm{s}}}{C_1} & 0 & 0 \\ \dfrac{(1-D_{\mathrm{s}})}{C_2} & \dfrac{(1-D_{\mathrm{s}})}{C_2} & 0 & \dfrac{-1}{C_2R_{\mathrm{eq}}} \end{bmatrix} \tag{12}$$

$$\boldsymbol{B}=\begin{bmatrix} \dfrac{1}{L_a} \\ 0 \\ 0 \\ 0 \end{bmatrix} \tag{13}$$

$$\boldsymbol{C}=[0 \quad 0 \quad 0 \quad 1] \tag{14}$$

$$\boldsymbol{D}=[0] \tag{15}$$

where R_{eq} is equivalent impedance at the dc link and D_{s} is the duty ratio of Sepic converter.

Similarly, the state-space matrices of the BIDC, state matrix '$\boldsymbol{A}_1$', input matrix '$\boldsymbol{B}_1$', output matrix '$\boldsymbol{C}_1$', feed forward matrix '$\boldsymbol{D}_1$' are found to be

$$\boldsymbol{A}_1=\begin{bmatrix} \dfrac{-(R_{\mathrm{lp}}+R_{\mathrm{dson}})}{L} & 0 & \dfrac{-(1-D_{\mathrm{BIDC}})}{L} \\ \dfrac{-1+2D_{\mathrm{BIDC}}}{C_L} & 0 & 0 \\ \dfrac{(1-D_{\mathrm{BIDC}})}{C_H} & 0 & \dfrac{-1}{C_HR_{\mathrm{eq1}}} \end{bmatrix} \tag{16}$$

$$\boldsymbol{B}_1=\begin{bmatrix} \dfrac{1}{L} \\ 0 \\ 0 \end{bmatrix} \tag{17}$$

$$\boldsymbol{C}_1=[0 \quad 0 \quad 1] \tag{18}$$

$$\boldsymbol{D}_1=[0] \tag{19}$$

where $L=(L_1/3)$, $R_{\mathrm{lp}}=(R_{L1}/3)$, R_{eq1} is equivalent impedance across capacitor C_H, R_{dson} the MOSFET turn on resistance, R_{L1} is the parasitic resistance of inductor, L_1 and D_{BIDC} is the duty ratio of BIDC.

Transfer functions of the converters are obtained from the above state-space models and they are combined to produce the overall transfer function of the proposed system. Frequency response of the proposed system exhibits the positive gain margin and phase margin which in turn indicates that the proposed system is stable.

Simulation studies of the proposed charger are carried out and the results are furnished in the following section.

6 Simulation studies and results

Simulink in the MATLAB software is used for the simulation studies of the proposed system. PV array is modelled using its classical equation [28, 29]. The Sepic and BIDC converter is modelled using power MOSFETs, inductors and capacitors available in SimPowerSystems Blockset in simulink library. Controller is developed using PWM generator, pulse generator, logic gates, comparator, multiplier and PI controller available in the Simulink library. PV array model is integrated with the

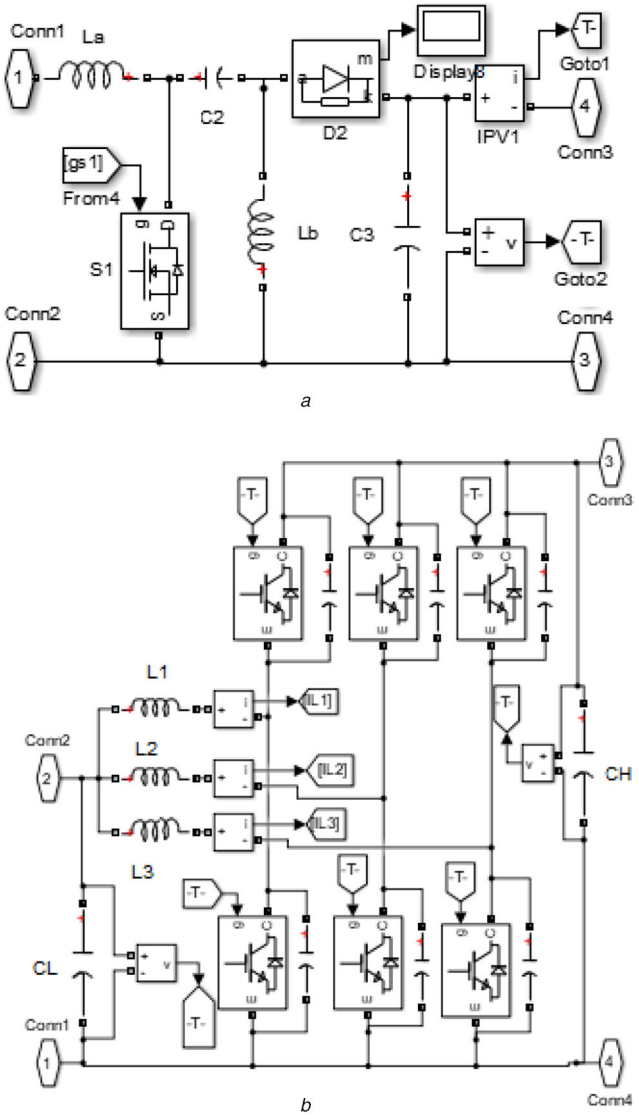

Fig. 6 *Simulation model of* ***(a)*** Sepic converter, ***(b)*** BIDC

developed sepic converter and BIDC along with the battery models available in Simulink library for developing the proposed charging system as shown in Fig. 5.

The developed simulation model of sepic converter and BIDC shown as subsystems in Fig. 5 are depicted in Figs. 6*a* and *b*, respectively.

The dynamic response of the system was investigated using the developed simulation model for PV array irradiation of 850, 100 and 500 W/m^2 in mode 1, mode 2 and mode 3, respectively. The simulation results showing PV array voltage and current waveforms along with the gate pulses to the auxiliary switches are depicted in Fig. 7. Irradiation waveforms are shown in the scale of 1 for 1000 W/m^2 in Fig. 7. Thus, both EV battery and backup battery gets charged simultaneously in this mode. Whereas at low irradiation of 100 W/m^2, the gate pulses of auxiliary switches, V_{gsb} and V_{gsc} are high and gate pulse, V_{gsa} is low as PV array power is insufficient for charging EV battery. Thus, the backup battery bank discharges through BIDC to charge EV battery in this mode.

During irradiation of 500 W/m^2, the auxiliary switches S_a and S_b are ON and switch S_c is OFF disconnecting backup battery from the system. Since PV array power is sufficient only for charging EV battery, backup battery is isolated and not charged in this mode. Fig. 7 shows that the gate pulses to the switch S_b is always high as the EV battery is constantly charged in all the three modes. If the EV battery is fully charged, EV battery is isolated from the

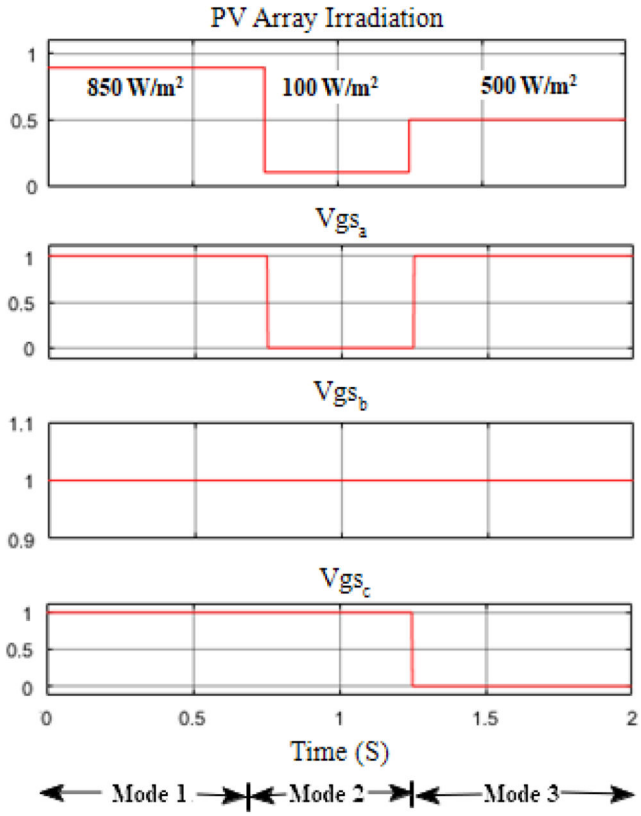

Fig. 7 *Waveforms of PV array irradiation and gate pulses to the auxiliary switches*

charging system by turning OFF Switch, S_b to avoid trickle charging of EV battery.

Fig. 8 depicts the simulated dynamic waveforms of PV array, dc link, EV battery and backup battery for the corresponding irradiation values. In mode 1, the PV array voltage, V_{PV} of 33.3 V is stepped down to the dc link voltage, V_{dc} of 28 V by sepic converter as shown in Figs. 8*a* and *b*. Increase in state of charge (SOC) of EV battery and its negative current shown in Fig. 8*c* indicates that the EV battery is charging in this mode. BIDC operates as boost converter in forward direction in this mode, boosting the dc link voltage, V_{dc} of 28 to 60.6 V to charge the backup battery with the increase in SOC as presented in Fig. 8*d*.

In mode 2 (during non-sunshine hours and low irradiation conditions), PV array is isolated resulting in PV array voltage, V_{PV} raising to its open circuit voltage of 37.25 V and PV array current, I_{PV} of 0 A, which is represented by the PV array voltage and current waveforms shown in Fig. 8*a*. During this period, BIDC operates in buck mode in reverse direction, stepping down the backup battery voltage to 27.32 V to charge the EV battery as shown in Fig. 8*c*. The positive current and decrease in SOC of backup battery shown in Fig. 8*d* indicates that the backup battery is discharged in this mode. At the end of this mode the backup battery voltage is reduced to 55.2 V from 60.6 V as depicted in Fig. 8*d*.

Whereas in mode 3, PV array voltage, V_{PV} of 31.81 V is step down to a dc link voltage, V_{dc} of 27.6 V to charge the EV battery as shown in Figs. 8*a* and *b*. In this mode also, SOC of EV battery is increasing and current is negative, indicating the charging of EV battery. In mode 3, as the backup battery is isolated from the charging system, backup battery voltage is maintained at its previous value of 55.2 V and current is reduced to zero as shown in Fig. 8*d*. Fig. 8*c* shows that the SOC of EV battery is increasing and its current is negative in all the three modes depicting that EV battery gets charged continuously either from PV array or from backup battery.

The interleaved inductor current waveforms of BIDC in all the modes of operation are shown in Fig. 9. The reversal of inductor current flow in mode 2 clearly indicates that the backup battery gets discharged in this mode and zero inductor current in the mode

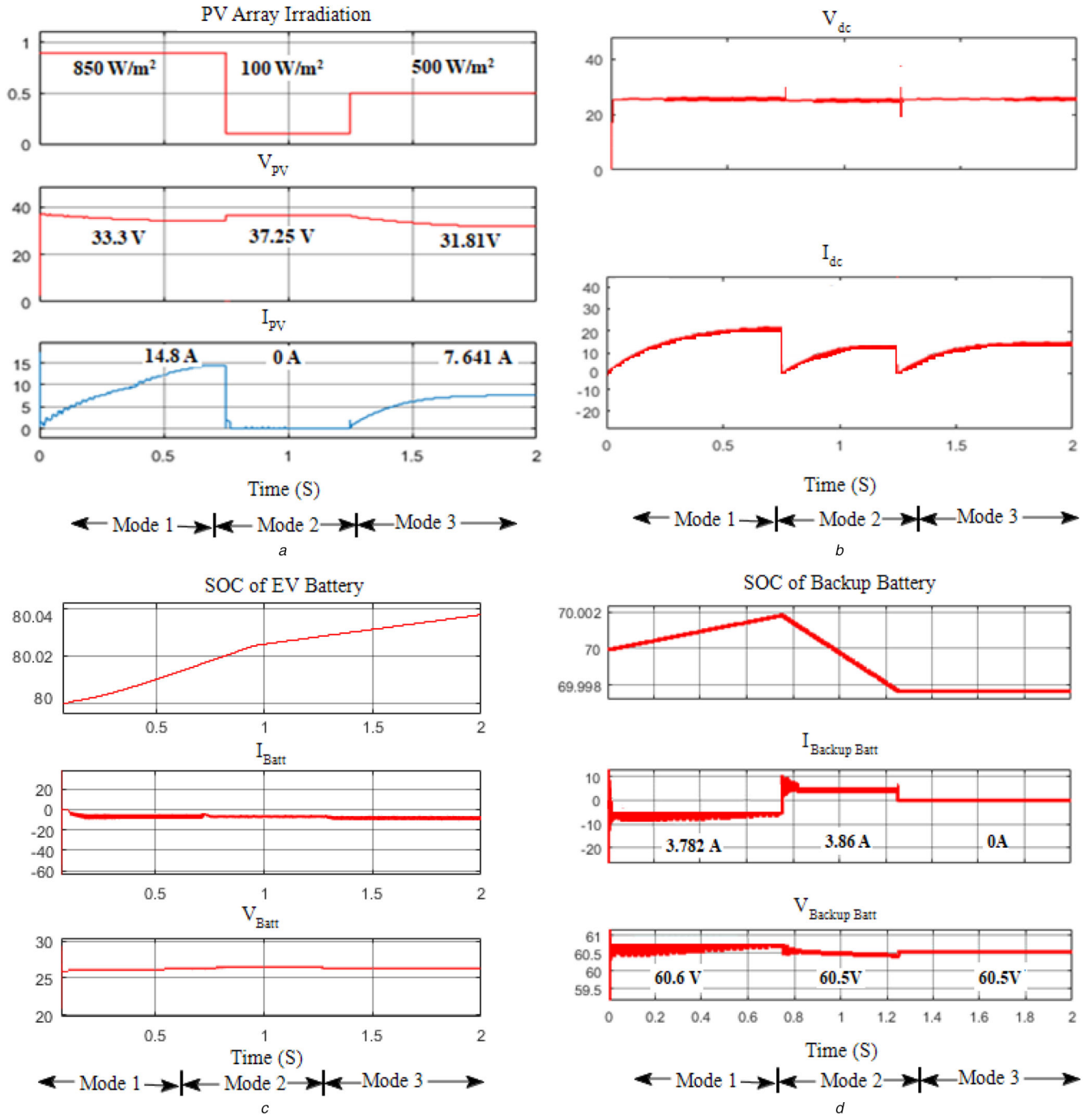

Fig. 8 *Waveforms of*
(a) PV array voltage, V_{PV} & PV array current, I_{PV}, ***(b)*** DC link voltage, V_{dc}, & current, I_{dc}, ***(c)*** EV battery SOC, EV battery current, I_{Batt} & EV battery voltage, V_{Batt}, ***(d)*** Backup battery SOC, backup battery current, $I_{Backup\ Batt}$ & backup battery voltage, $V_{Backup\ Batt}$

3 indicates that the BIDC is disconnected from the charger. To validate the simulation studies, hardware prototype is developed and tested and their results are furnished in the following section.

7 Experimental setup and results

The hardware prototype of the proposed EV battery charger was fabricated and tested in the laboratory. The experimental setup was tested with Magna programmable dc supply as the input power source being used as PV array (two panels with open circuit voltage, V_{oc} of 37.25 V and short circuit current, I_{sc} of 8.75 A are connected in parallel).

MOSFET IRF540 (100 V, 28 A), Diode RHRP30120 (1200 V, 30 A), inductors of 1 mH/20 A and capacitors of 1000 µF/250 V and 600 µF/150 V are used to fabricate sepic converter. BIDC is fabricated using the similar rated MOSFET, snubber capacitors of 0.1 µF/63 V, Inductors of 85 µH/15 A and capacitors of 1 µF/450 V and 100 µF/160 V. The gate pulses of 25 kHz switching frequency are fed to the MOSFET switches of sepic converter and BIDC using PIC16F876A microcontroller and IR2130 driver circuit. Lead acid batteries (2 batteries each of 12 V, 35 Ah are connected in series) are used as EV battery and 5 batteries each of 12 V, 100 Ah are connected in series for backup battery bank. The components specification of the proposed system is furnished in Table 1.

Also, the experimental investigation is carried out in rapid control prototyping (RCP) methodology in OPAL-RT Real time simulator OP4500. Controller is designed in the MATLAB/Simulink software in the RT Lab environment. The input signals, V_{in} and I_{in} are sensed using sensing instrument available in the laboratory and provided as analogue input to the controller through analogue input ports of OP4500 using DB37 connector. The gate pulses are generated from OPAL-RT and fed to the MOSFET switches using IR2130 driver circuit through analogue output ports

of OP4500. The photograph of the experimental setup is shown in Fig. 10.

The experimental results of the proposed charging system in different modes are shown in Figs. 11–13. Figs. 11*a* and *b* show

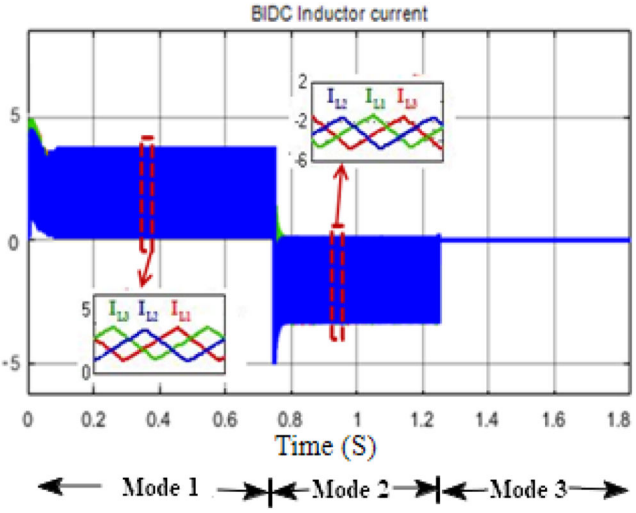

Fig. 9 *Inductor current waveforms of BIDC*

Table 1 Hardware specifications

Components	Specifications	No. of components
MOSFET, IRF540	100 V, 28 A	7
diode, RHRP30120	1200 V, 30 A	1
inductors, L_a & L_b	1 mH, 20 A	2
capacitor, C_a	1000 μF, 250 V	1
capacitor, C_b	600 μF, 150 V	1
microcontroller	Atmega 32	2
gate Driver	IR2110	6
DIODE RHRP8120	500 V, 10 A	6
inductors, L_1, L_2 & L_3	85 μH/15 A	3
capacitor, C_L	1 μF/ 450 V	1
capacitor, C_H	100 μF/160 V	1

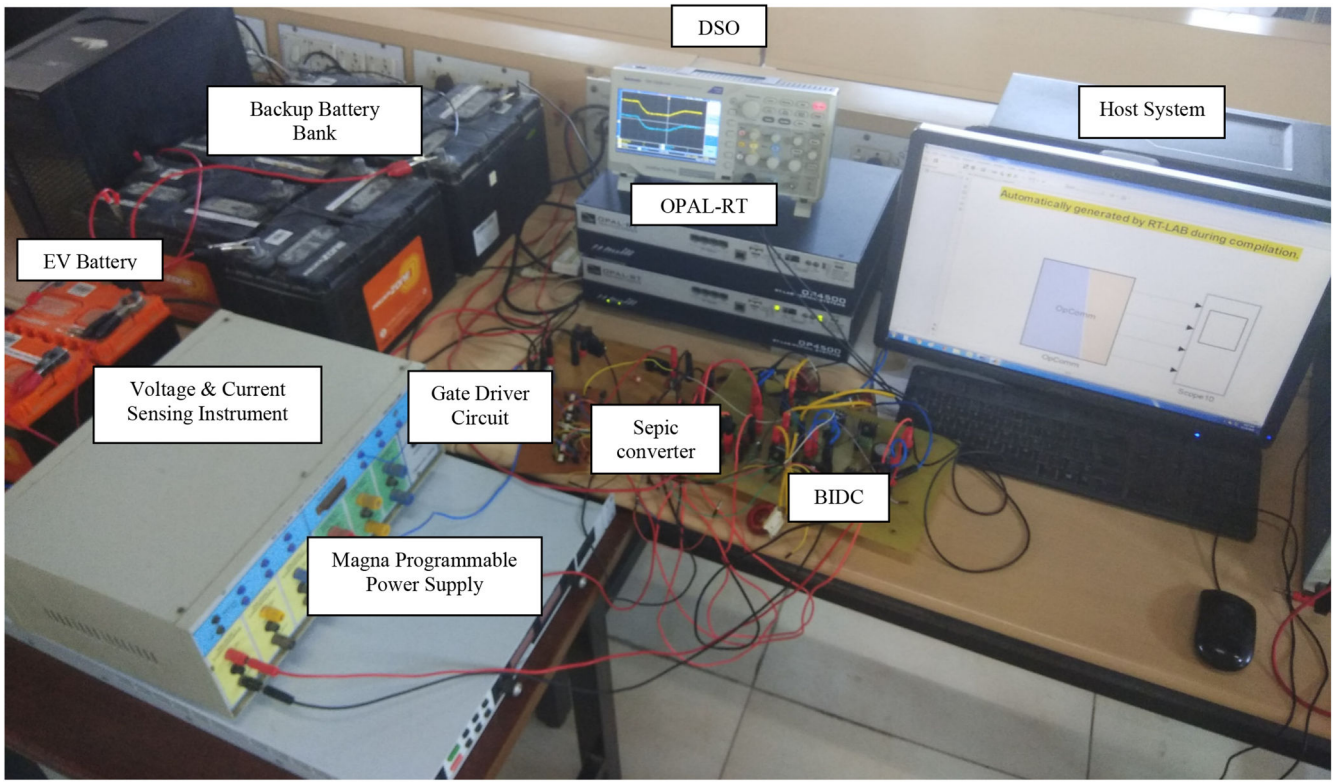

Fig. 10 *Photograph of the experimental setup*

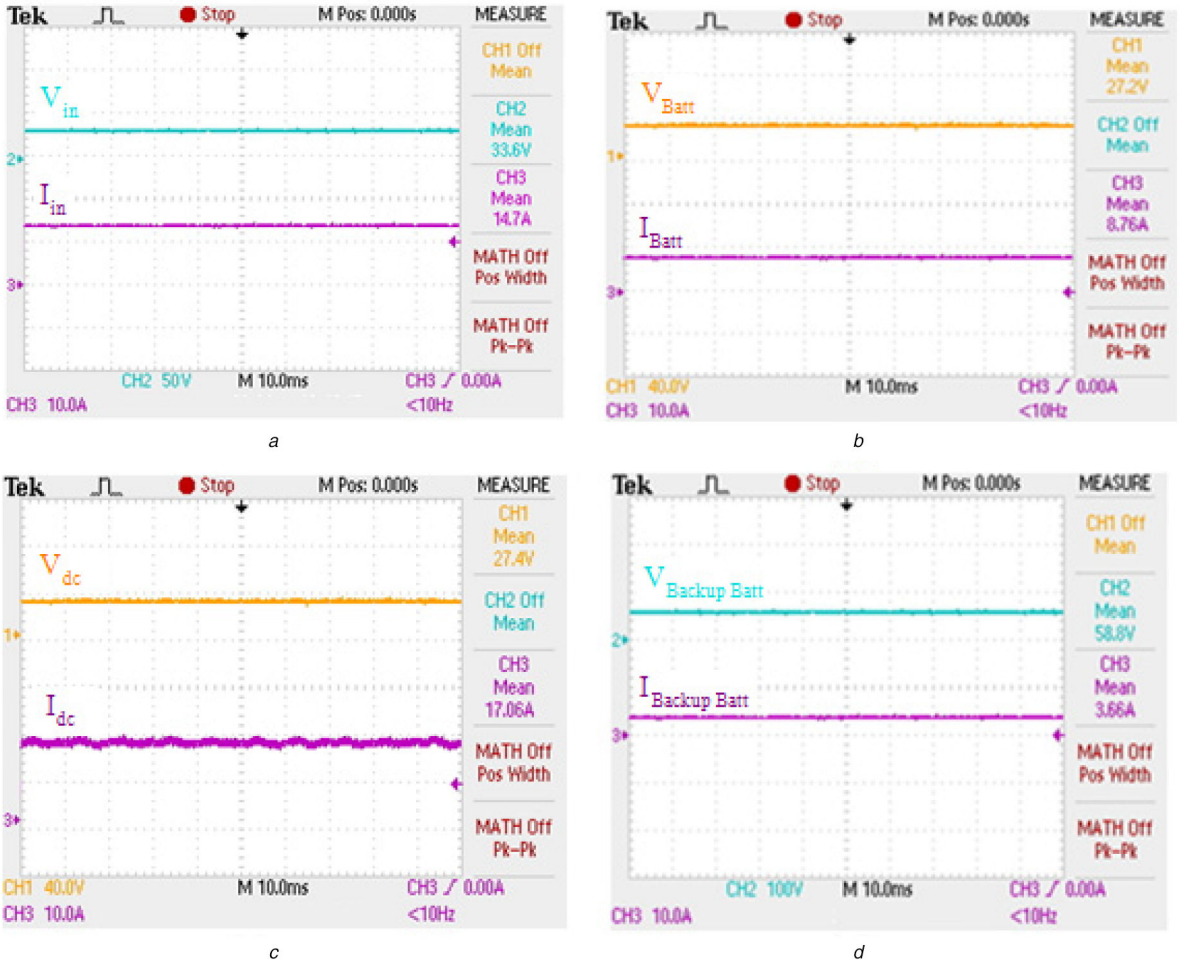

Fig. 11 *Mode 1 experimentation waveforms of*
(a) Sepic input, ***(b)*** Sepic output, ***(c)*** EV battery, ***(d)*** Backup battery

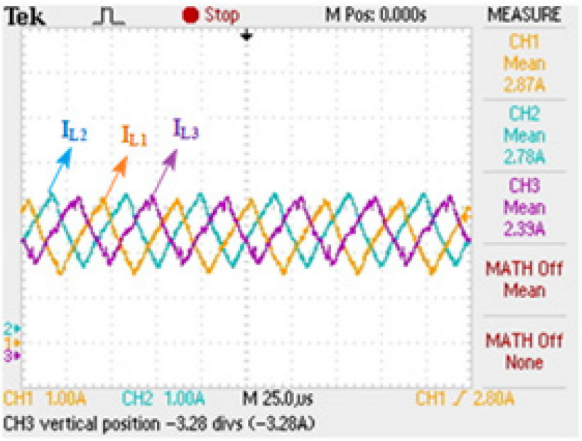

Fig. 12 *Inductor current waveforms of BIDC in mode 1*

that the input voltage, V_{in} of 33.6 V was bucked to a dc link voltage, V_{dc} of 27.4 V by the sepic converter to charge both EV battery and backup battery. Fig. 11*c* shows the waveforms of EV battery voltage, V_{Batt} of 27.2 V and current, I_{Batt} of 8.76 A. In this mode, BIDC operates in boost mode with the duty ratio of 0.53 boosting the dc link voltage, V_{dc} of 27.4 V to charge the backup battery.

The backup battery voltage, $V_{BackupBatt}$ of 58.8 V is obtained as shown in Fig. 11*d* and the waveforms of inductor currents of the BIDC in this mode is shown in Fig. 12. In mode 1, out of 467 W input power, 238 W power is supplied to the EV battery and 215 W is supplied to the backup battery.

In mode 2, input dc supply along with sepic converter is isolated from the charging system and the backup battery discharges through BIDC to charge EV battery. In this mode, BIDC operates in buck mode in the reverse direction with the duty ratio of 0.41 for stepping down the backup battery voltage, $V_{BackupBatt}$ of 60.7 V and the EV battery voltage, V_{Batt} of 25 V is obtained as shown in Figs. 13*a* and *b*, respectively and Fig. 13*c* shows the waveforms of inductor currents of BIDC. In this mode, out of 228 W of backup battery power, 222 W is supplied to the EV battery contributing to the charging system efficiency of 97%.

In mode 3, backup battery is disconnected along with the BIDC from the charging system and the EV battery alone gets charged from the input source. The input voltage, V_{in} of 28.6 V is stepped

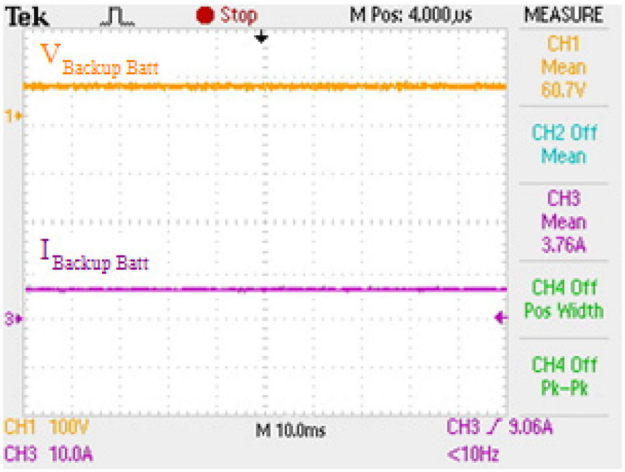

a

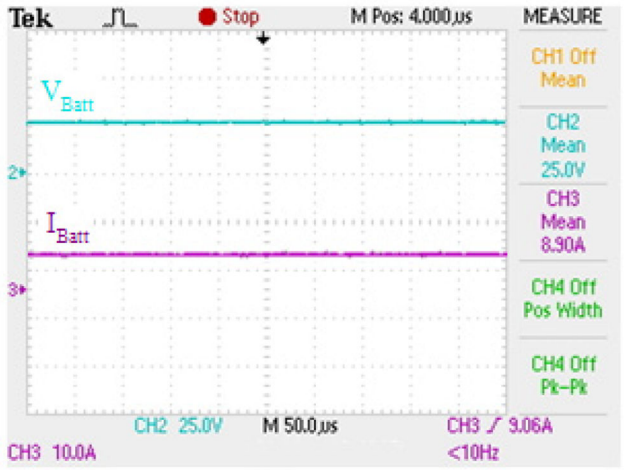

b

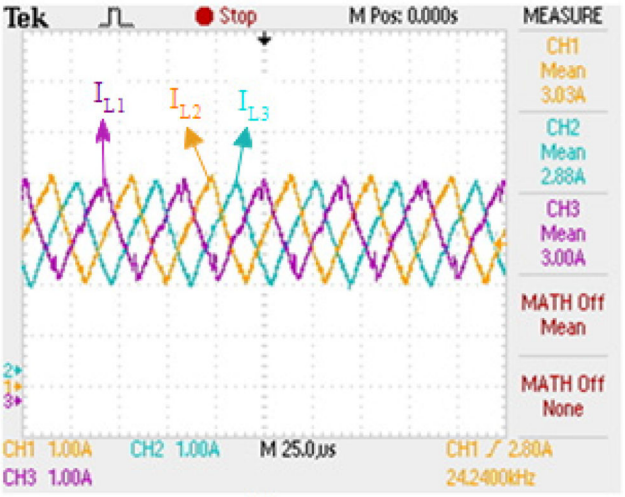

c

Fig. 13 *Mode 2 Experimentation waveforms of*
(a) Backup battery, ***(b)*** EV battery, ***(c)*** BIDC Inductor currents

down and EV battery voltage, V_{Batt} of 27.2 V is obtained as shown in Fig. 14. In both simulation and experimentation, the average efficiency of the charging system in all the three modes was found to be ~96%. From the waveforms shown in Section 5 and Section 6, it is evident that the experimentation results are in tune with the simulation results proving the effectuality of the charging system.

The dynamic response of the system was depicted in Fig. 15. The input voltage and current waveforms are shown in Fig. 15*a* with the mode transition and the corresponding EV battery voltage and current waveforms and backup battery voltage and current waveforms are shown in Figs. 15*b* and *c*, respectively. From

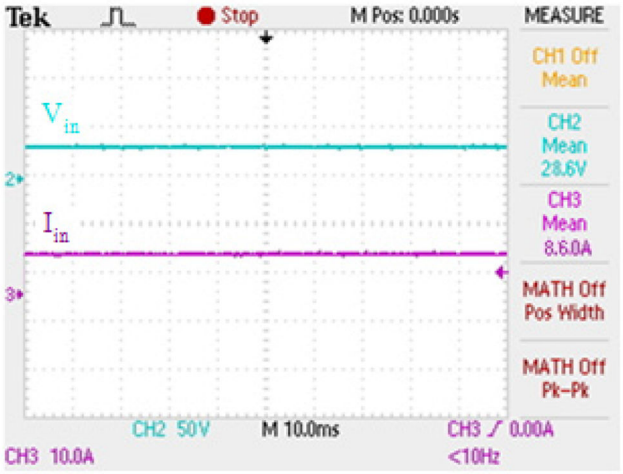

a

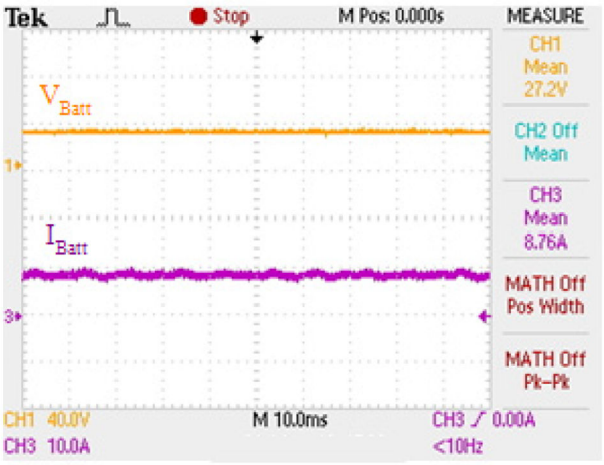

b

Fig. 14 *Experimentation waveforms of*
(a) Sepic input, ***(b)*** EV battery in Mode 3

Figs. 15*a–c*, it is clear that in mode 1, input power is used to charge both EV battery and backup battery. In mode 2, as the input power is insufficient to charge EV battery, input source is isolated from the system which is indicated by zero input current in Fig. 15*a* and backup battery is discharged to supply power to the EV battery which is indicated by the negative backup battery current in Fig. 15*c*. In mode 3, input power is sufficient enough to charge EV battery only and hence the backup battery is isolated from the system which is indicated by zero backup battery current in Fig. 15*c*. Fig. 15*b* clearly depicts that the EV battery is charged with constant voltage of 27 V approximately in all the 3 modes.

8 Conclusion

In this paper, an off-board EV battery charging system fed from PV array is proposed. This paper discusses the flexibility of the system to charge the EV battery constantly irrespective of the irradiation conditions. The system is designed and simulated in Simulink environment of the MATLAB software. The hardware prototype is fabricated and tested in laboratory for the three modes of operation of the proposed charging system separately and the results are furnished. In OPAL-RT Real time simulator OP4500, experimental investigation is carried out in RCP methodology and the dynamic response of the system is furnished both in simulation and experimental investigation. Correlation between the simulation and experimental results emphasise the effectiveness of the proposed charger.

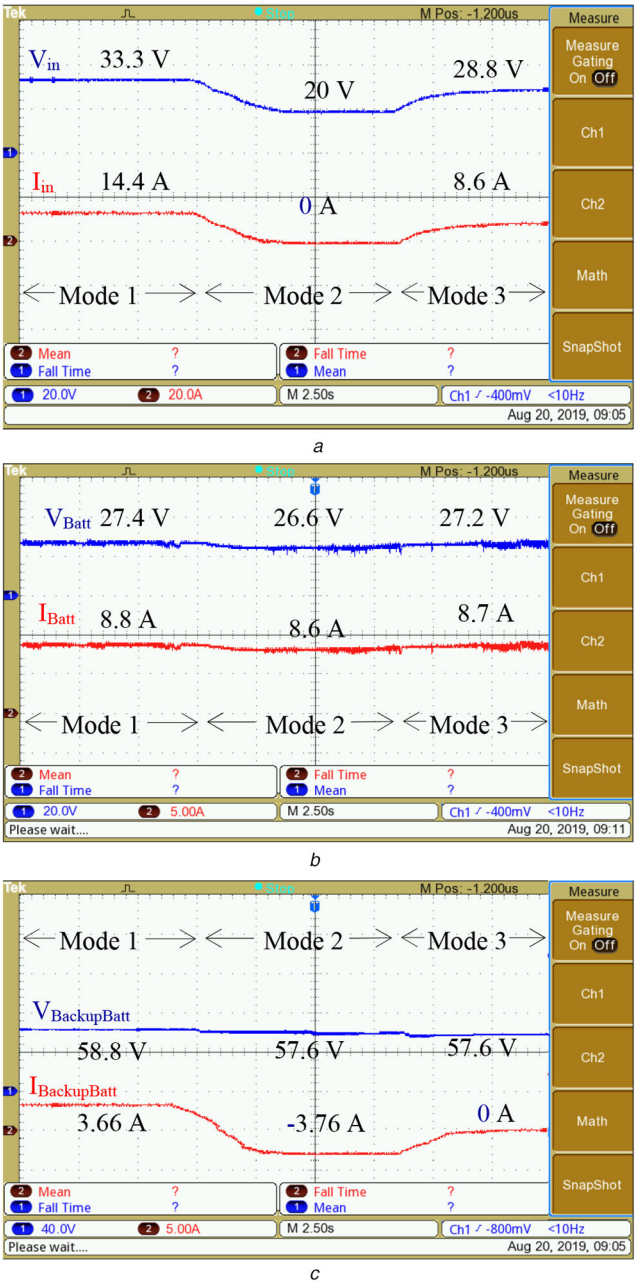

Fig. 15 *Dynamic response of the system showing the Experimental investigation waveforms of*

(a) Input voltage and current, ***(b)*** EV battery voltage and current, ***(c)*** Backup battery voltage and current

9 References

[1] Santhosh, T.K., Govindaraju, C.: 'Dual input dual output power converter with one-step-ahead control for hybrid electric vehicle applications', *IET Electr. Syst. Transp.*, 2017, **7**, (3), pp. 190–200

[2] Shukla, A., Verma, K., Kumar, R.: 'Voltage-dependent modelling of fast charging electric vehicle load considering battery characteristics', *IET Electr. Syst. Transp.*, 2018, **8**, (4), pp. 221–230

[3] Wirasingha, S.G., Emadi, A.: 'Pihef: plug-in hybrid electric factor', *IEEE Trans. Veh. Technol.*, 2011, **60**, pp. 1279–1284

[4] Kirthiga, S., Jothi Swaroopan, N.M.: 'Highly reliable inverter topology with a novel soft computing technique to eliminate leakage current in grid-connected transformerless photovoltaic systems', *Comput. Electr. Eng.*, 2018, **68**, pp. 192–203

[5] Badawy, M.O., Sozer, Y.: 'Power flow management of a grid tied PV-battery system for electric vehicles charging', *IEEE Trans. Ind. Appl.*, 2017, **53**, pp. 1347–1357

[6] Van Der Meer, D., Chandra Mouli, G.R., Morales-Espana Mouli, G., *et al.*: 'Energy management system with PV power forecast to optimally charge EVs at the workplace', *IEEE Trans. Ind. Inf.*, 2018, **14**, pp. 311–320

[7] Xavier, L.S., Cupertino, A.F., Pereira, H.A.: 'Ancillary services provided by photovoltaic inverters: single and three phase control strategies', *Comput. Electr. Eng.*, 2018, **70**, pp. 102–121

[8] Krithiga, S., Ammasai Gounden, N.: 'Investigations of an improved PV system topology using multilevel boost converter and line commutated inverter with solutions to grid issues', *Simul. Model. Pract. Theory*, 2014, **42**, pp. 147–159

[9] Sujitha, N., Krithiga, S.: 'RES based EV battery charging system: a review', *Renew. Sustain. Energy Rev.*, 2017, **75**, pp. 978–988

[10] Farzin, H., Fotuhi-Firuzabad, M., Moeini-Aghtaie, M.: 'A practical scheme to involve degradation cost of lithium-ion batteries in vehicle-to-grid applications', *IEEE Trans. Sustain. Energy*, 2016, **7**, pp. 1730–1738

[11] Zubair, R., Ibrahim, A., Subhas, M.: 'Multiinput DC–DC converters in renewable energy applications – an overview', *Renew. Sustain. Energy Rev.*, 2015, **41**, pp. 521–539

[12] Duong, T., Sajib, C., Yuanfeng, L., *et al.*: 'Optimized multiport dc/dc converter for vehicle drive trains: topology and design optimization', *Appl. Sci.*, 2018, **1351**, pp. 1–17

[13] Santhosh, T.K., Natarajan, K., Govindaraju, C.: 'Synthesis and implementation of a multi-port dc/dc converter for hybrid electric vehicles', *J. Power Electron.*, 2015, **15**, (5), pp. 1178–1189

[14] Hongfei, W., Peng, X., Haibing, H., *et al.*: 'Multiport converters based on integration of full-bridge and bidirectional dc–dc topologies for renewable generation systems', *IEEE Trans. Ind. Electron.*, 2014, **61**, pp. 856–869

[15] Shi, C., Khaligh, A.: 'A two-stage three-phase integrated charger for electric vehicles with dual cascaded control strategy', *IEEE J. Emerging Sel. Topics Power Electron.*, 2018, **6**, (2), pp. 898–909

[16] Chiang, S.J., Shieh, H., Chen, M.: 'Modeling and control of PV charger system with SEPIC converter', *IEEE Trans. Ind. Electron.*, 2009, **56**, (11), pp. 4344–4353

[17] Falin, J.: 'Designing DC/DC converters based on SEPIC topology', *Analog Appl. J.*, 2008, **4Q**, pp. 18–23. Available at https://e2echina.ti.com/cfs-file/__key/telligent-evolution-components-attachments/13-112-00-00-00-00-58-20/Designing-DC-DC-converters-based-on-SEPIC-topology.pdf

[18] Banaei, M.R., Sani, S.G.: 'Analysis and implementation of a new SEPIC-based single-switch buck–boost DC–DC converter with continuous input current', *IEEE Trans. Power Electron.*, 2018, **33**, (12), pp. 10317–10325

[19] Singh, A.K., Pathak, M.K.: 'Single-stage ZETA-SEPIC-based multifunctional integrated converter for plug-in electric vehicles', *IET Electr. Syste. Transp.*, 2018, **8**, (2), pp. 101–111

[20] Du, Y., Zhou, X., Bai, S., *et al.*: 'Review of non-isolated bi-directional DC-DC converters for plug-in hybrid electric vehicle charge station application at municipal parking decks'. 2010 Twenty-Fifth Annual IEEE Applied Power Electronics Conf. Exposition, Palm Springs, CA, USA., 2010, pp. 1145–1151

[21] Kwon, M., Oh, S., Choi, S.: 'High gain soft-switching bidirectional DC–DC converter for eco-friendly vehicles', *IEEE Trans. Power Electron.*, 2014, **29**, pp. 1659–1666

[22] Mirzaei, A., Jusoh, A., Salam, Z., *et al.*: 'Analysis and design of a high efficiency bidirectional DC–DC converter for battery and ultracapacitor applications', *Simul. Model. Pract. Theory*, 2011, **19**, pp. 1651–1667

[23] Han, J.T., Lim, C.-S., Cho, J.-H., *et al.*: 'A high efficiency non-isolated bidirectional DC-DC converter with zero-voltage-transition'. 2013 - 39th Annual Conf. IEEE Industrial Electronics Society, 2013, pp. 198–203

[24] Zhang, J., Lai, J.-S., Kim, R.-Y., *et al.*: 'High-power density design of a soft-switching high-power bidirectional DC–DC converter', *IEEE Trans. Power Electron.*, 2007, **22**, pp. 1145–1153

[25] Paul, A., Subramanian, K., Sujitha, N.: 'PV-based off-board electric vehicle battery charger using BIDC', *Turk. J. Electr. Eng. Comput. Sci.*, 2019, **27**, (4), pp. 2850–2865

[26] Sree, L., Umamaheswari, M.G.: 'A Hankel matrix reduced order SEPIC model for simplified voltage control optimization and MPPT', *Sol. Energy*, 2018, **170**, pp. 280–292

[27] Zhang, J.: 'Bidirectional DC-DC power converter design optimization, modeling and control'. Dissertation, the faculty of the Virginia Polytechnic Institute and State University, Virginia Polytechnic Institute and State University, 2008

[28] Gounden, N.G.A., Krithiga, S.: 'Power electronic configuration for the operation of PV system in combined grid-connected and stand-alone modes', *IET Power Electron.*, 2014, **7**, pp. 640–647

[29] Arul Daniel, S., Ammasai Gounden, N.: 'A novel hybrid isolated generating system based on PV fed inverter assisted wind driven induction generators', *IEEE Trans. Energy Convers.*, 2004, **19**, (2), pp. 416–422